Distribution of hematopoietic stem cells in the bone marrow according to regional hypoxia

Kalindi Parmar*†, Peter Mauch*‡§, Jo-Anne Vergilio¶, Robert Sackstein‖, and Julian D. Down**

*Department of Radiation Oncology, Dana–Farber Cancer Institute, Departments of ‡Radiation Oncology and ¶Pathology, and ‖Departments of Dermatology and Medicine, Brigham and Women's Hospital, Harvard Medical School, Boston, MA 02115; and **Genetix Pharmaceuticals, Inc., Cambridge, MA 02139

Communicated by Stephen J. Elledge, Harvard Medical School, Boston, MA, February 9, 2007 (received for review November 17, 2006)

The interaction of stem cells with their bone marrow microenvironment is a critical process in maintaining normal hematopoiesis. We applied an approach to resolve the spatial organization that underlies these interactions by evaluating the distribution of hematopoietic cell subsets along an *in vivo* Hoechst 33342 (Ho) dye perfusion gradient. Cells isolated from different bone marrow regions according to Ho fluorescence intensity contained the highest concentration of hematopoietic stem cell (HSC) activity in the lowest end of the Ho gradient (i.e., in the regions reflecting diminished perfusion). Consistent with the ability of Ho perfusion to simulate the level of oxygenation, bone marrow fractions separately enriched for HSCs were found to be the most positive for the binding of the hypoxic marker pimonidazole. Moreover, the *in vivo* administration of the hypoxic cytotoxic agent tirapazamine exhibited selective toxicity to the primitive stem cell subset. These data collectively indicate that HSCs and the supporting cells of the stem cell niche are predominantly located at the lowest end of an oxygen gradient in the bone marrow with the implication that regionally defined hypoxia plays a fundamental role in regulating stem cell function.

Hoechst perfusion | stem cell niche | oxygen gradient | pimonidazole | tirapazamine

Mammalian hematopoiesis in the adult originates in the bone marrow where a rare population of quiescent stem cells gives rise to expanding populations of committed progenitors that then replenish all of the blood cell lineages throughout the lifetime of the organism. The proliferative potential of hematopoietic stem cells (HSCs) is thus considerable being endowed with the special ability to perpetuate themselves by self-renewal. Although the exogenous signals that influence the choice between self-renewal and differentiation of HSCs are not completely defined, they are generally thought to reside in discrete microenvironmental domains within the bone marrow that are termed "niches" (1).

Functionally, HSCs in mice are often defined in transplantation experiments by their ability to engraft and maintain hematopoiesis in lethally irradiated recipients (2). Although no studies have directly investigated the distribution of actual long-term repopulating HSCs within bone marrow, a few have suggested that at least some hematopoietic cells reside in close proximity to the endosteal surface of the bone and that hematopoietic differentiation proceeds radially toward the longitudinal axis of the marrow (1, 3, 4). Recent genetic studies have confirmed that endosteal osteoblasts are a crucial cellular element of HSC niches (5, 6). Calvi *et al.* (5) found a parallel and selective expansion of HSCs when they increased the numbers of osteoblasts in bone marrow using parathyroid hormone and further implicated the 'Notch' pathway in signal transduction. Zhang *et al.* (6) showed that depleting osteoblasts of the receptor for bone morphogenic protein also caused an elevation in both osteoblast and HSC numbers and provided additional evidence that adherence of these two cell types via N-cadherin could play a role in defining the HSCs niche. Finally, Arai *et al.* (7) demonstrated that a hematopoietic cell subset expressing the receptor tyrosine kinase Tie2 are mostly confined to the Hoechst (Ho) dye effluxing "side population" (SP) phenotype and adhere to osteoblasts. They also provided evidence that the interaction of Tie2 with its ligand Angiopoietin-1 determines the maintenance of HSCs in a quiescent state.

Oxygen, or lack thereof, plays a well-known physiological role in cellular respiration but its impact in the regulation of HSC function in relation to the supporting niche has received relatively little attention. Most *in vivo* studies in this area have been directed toward examining the state of hypoxia in pathological conditions such as those encountered in solid tumors. According to the classical "Thomlinson and Gray model," chronically hypoxic and noncycling tumor cells exist at a limiting distance of 100–150 μm away from blood vessels (8). The existence of hypoxia has subsequently been shown to be common among a number of different tumor types and has thus formed the conceptual basis for intense research that attempts to both selectively target hypoxic cells in cancer treatment and to establish prognostic indicators of clinical response (9, 10). Although hypoxia is not generally believed to be present in most healthy normal tissues, bone marrow may represent a somewhat unique tissue type given its complicated hierarchical organization emanating from a small population of resting stem cells. To date, little is known about the distribution and relationship of hematopoietic cells with respect to blood vessels or blood supply. A number of reports have shown that hematopoiesis can be improved ex-vivo by maintaining the cell cultures at levels of between 1% and 3% O_2 (11–13) but the relevance of such findings to the *in vivo* situation is uncertain. Chow *et al.* (14) used mathematical modeling of pO_2 distributions in the bone marrow and speculated that stem cells are located at the region with very low pO_2 levels (almost anoxic) because this prevents oxygen radicals from damaging these important cells. Although such modeling is certainly provocative, the inaccessibility of bone marrow to direct noninvasive oxygen measurements has become a major hurdle to formal experimental investigation. Nonetheless, the increasing availability of hypoxic cell markers together with routine methods for measuring blood perfusion as applied in tumor biology now provides an opportunity to re-explore the existence of oxygen gradients within the bone marrow. Here, we provide direct evidence that primitive hematopoietic cells in the bone marrow are sequestered in a hypoxic

Author contributions: K.P., P.M., R.S., and J.D.D. designed research; K.P. and J.D.D. performed research; J.-A.V. contributed new reagents/analytic tools; K.P. and J.D.D. analyzed data; and K.P. and J.D.D. wrote the paper.

The authors declare no conflict of interest.

Abbreviations: HSC, hematopoietic stem cell; Ho, Hoechst; SP, side population; CAFC, cobblestone area-forming cell; PIM, pimonidazole.

†To whom correspondence may be addressed at: Department of Radiation Oncology, Jimmy Fund Building, Room 518B, Dana–Farber Cancer Institute, 44 Binney Street, Boston, MA 02115. E-mail: kalindi_parmar@dfci.harvard.edu.

§To whom correspondence may be addressed at: Department of Radiation Oncology, ASB1-L2, Brigham and Women's Hospital, 75 Francis Street, Boston, MA 02115. E-mail: pmauch@lroc.harvard.edu.

This article contains supporting information online at www.pnas.org/cgi/content/full/0701152104/DC1.

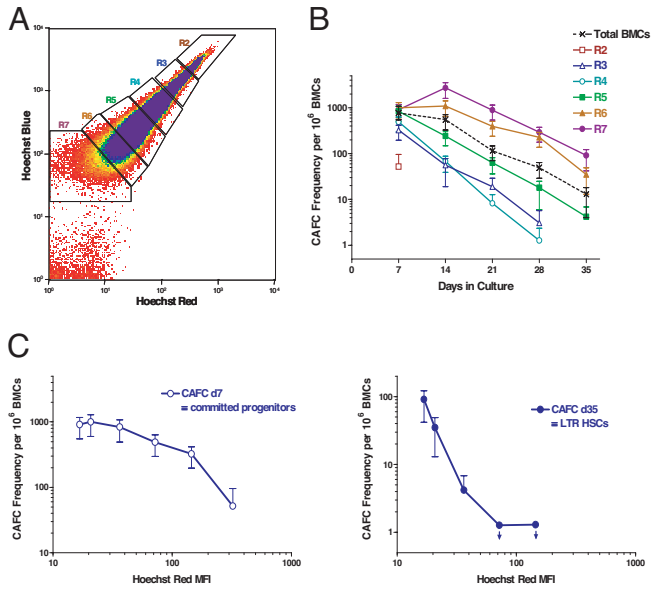

Fig. 1. Separation of different bone marrow cell (BMC) fractions according to a Ho dye diffusion gradient. (*A*) Blue versus red fluorescence intensity of BMCs after i.v. infusion of Ho dye (0.8 mg per mouse at 5 and 10 min before killing) with R2-R7 gates representing sorted cell fractions of diminishing fluorescence. (*B*) CAFC frequencies versus time in culture for the different cell fractions. (*C*) Early- and late-forming CAFC frequencies as a function of Ho red mean fluorescence intensity (MFI) determined from analysis of postsorted cells. Downward arrows indicate that the CAFC frequencies were below the limit of detection.

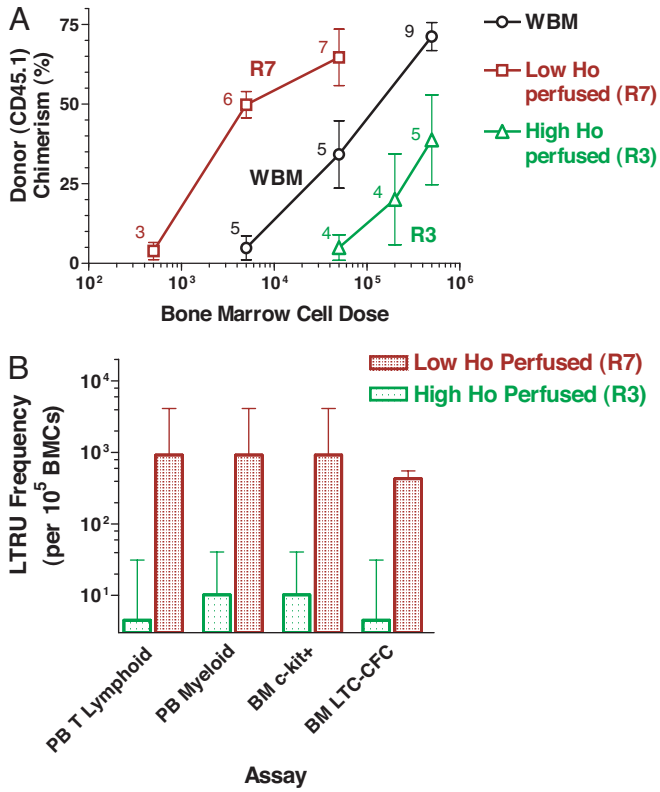

Fig. 2. Long-term repopulation for donor cells (CD45.1) sorted from high (R3) and low (R7) Ho-perfused bone marrow. Sorted bone marrow cells from donor (CD45.1) mice were transplanted into 10 Gy irradiated recipients (CD45.2) along with 200,000 recipient-type, non-SP cells to provide for short-term repopulation. Donor cell chimerism in the recipient mice was analyzed at 18 weeks and 12–14 months posttransplant. (*A*) Myeloid engraftment in the blood after 18 weeks posttransplant is shown. The number of mice for each cell dose group is indicated. The frequencies of repopulating cells (LTRUs) capable of producing >50% myeloid engraftment with 95% confidence limits (L-Calc program; Stem Cell Technologies) were 67 (27–166), 4.5 (2–10), and 1.1 (0.34–3.35) per 10^6 sorted cells from R7, whole Ho gradient (WBM), and R3 regions, respectively. (*B*) High (R3) versus low (R7) Ho dye perfused bone marrow populations for frequency of *in vivo* 12–14 month posttransplant LTRUs. Frequencies of donor cell chimerism in peripheral blood (PB) T cells, PB myeloid cells, bone marrow (BM) c-kit$^+$ cells, and BM LTC-CFC are shown. Error bars represent 95% confidence limits.

microenvironment implying that low oxygen levels play a fundamental role in the maintenance of normal stem cell function.

Results

Distribution of Different Hematopoietic Subsets Along a Ho Dye Perfusion Gradient. A number of previous animal studies have used i.v. injection of the diffusible Ho dye to visualize, with fluorescence microscopy applied to tissue sections, the perfusion of solid tumors in relation to hypoxia. Most of these reports describe the location of hypoxic cells at a relatively constant distance from blood vessels and in regions with low Ho staining (15–17). The Ho dye diffusion gradient can, however, be better quantitated by using flow cytometric analysis of disaggregated tissue and this methodology allows one to correlate the intensity of Ho staining with the degree of oxygenation (18, 19). We therefore adopted a similar approach by employing *in vivo* Ho uptake in bone marrow cells as an indicator of oxygen perfusion.

To measure Ho perfusion *in vivo*, mice were i.v. injected with two doses of Ho dye at 10 and 5 min before bone marrow harvesting, a period that was optimized for Ho uptake. Peripheral blood leukocytes and thymocytes as well as bone marrow cells were analyzed for Ho fluorescence on a logarithmic scale. Fig. 1*A* shows a wide distribution of Ho staining for bone marrow that covers 3 logs of fluorescence intensity and thereby forms an evident gradient. This contrasts with the higher and narrower distribution of fluorescence in the well-oxygenated blood leukocytes where Ho perfusion is expected to be the highest and with the very low levels of staining in the thymus where the majority of cells exist in a relatively hypoxic state [see supporting information (SI) Fig. 5]. The variation in Ho fluorescence among bone marrow cells mostly reflects *in vivo* perfusion of the dye as these differences were far too large to be accounted for by differences in DNA content. SP cells in the bone marrow are known to efflux Ho dye *in vitro* (20). We determined that the short time between Ho injection and marrow harvesting (10 min at 37°C) was insufficient for active dye efflux *in vitro* and remained unaffected by addition of the efflux inhibitor reserpine (SI Fig. 6).

We then assessed how different hematopoietic cell subsets were distributed along the Ho dye perfusion gradient in the bone marrow. Cells from six different regions of the Ho gradient were isolated and evaluated for hematopoietic activity in the cobblestone area-forming cell (CAFC) assay. CAFC frequencies at shorter (days 7–14) and longer (days 28–35) times in culture were used to measure relatively mature and primitive hematopoietic cell populations, respectively. As shown in Fig. 1*B*, there was a diminution of CAFCs in the highest Ho stained cells (R2), presumably because much of this fraction consists of circulating blood. Among the other sorted fractions, short-term (day 7) CAFC frequencies were similar but the curves diverged at later culture times according to their position along the gradient with the lowest Ho fluorescence giving the highest concentration of long-term (day 35) CAFCs (Fig. 1 *B* and *C*). No toxicity of the Ho dye was evident in a separate experiment comparing the CAFC frequencies harvested from mice with or without Ho administration (data not shown).

To assess the *in vivo* repopulating ability of the cells in the Ho gradient, the cells from the far ends of this gradient within bone

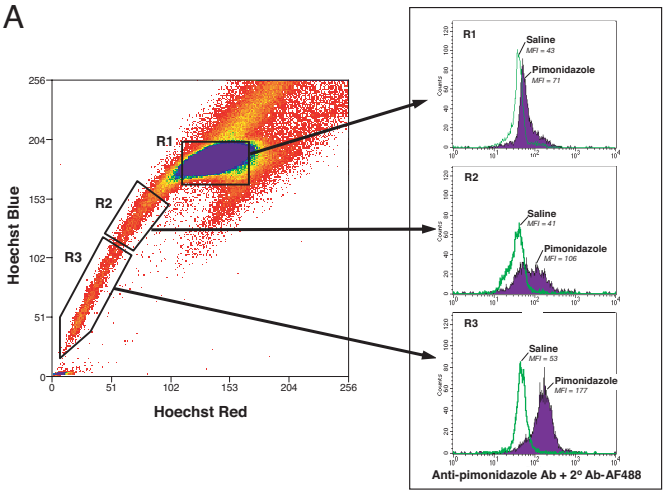

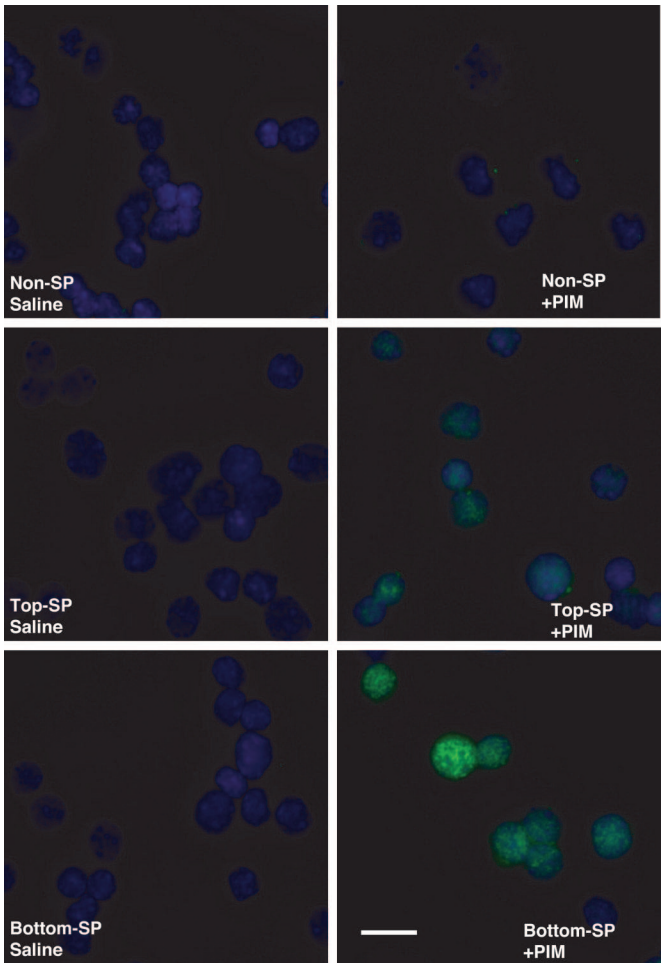

Fig. 3. PIM adducts *in vivo* in bone marrow SP cells. Mice were injected with saline or 120 mg/kg PIM ($n = 5$), and after 3 h, bone marrow samples were collected and subjected to Ho staining *in vitro* to isolate SP cells. Representative PIM staining of SP and non-SP cells in the bone marrow is shown. Three different regions of bone marrow cells based on Ho dye efflux, non-SP (R1), top SP (R2), and bottom SP (R3) were sorted. The sorted cells were analyzed for PIM binding by using flow cytometry (*A*) as well as immunofluorescence microscopy (*B*). (*A*) For flow cytometric analysis of PIM binding, the sorted cells were fixed and intracellularly stained by using anti-PIM primary antibody and a goat anti-mouse IgG F(ab′)$_2$ Alexa Fluor 488 secondary antibody. Similar positive staining of SP cells were obtained in two other separate experiments, including cells stained by using the FITC-conjugated anti-PIM antibody. (*B*) For visualization of PIM binding by microscopy, cytospin slides of non-SP, top SP, and bottom ''tip'' SP were immunostained for the adduct. Representative images stained for PIM (green) and nucleus (DAPI, blue) are shown. (Scale bar: 10 μM.)

marrow (R3 and R7 regions) were isolated from CD45.1 congenic mice and transplanted at varying cell doses into lethally irradiated CD45.2 recipients. Assessment of donor-type blood cell chimerism at 18 weeks posttransplant showed results that were in accordance with the primitive CAFC frequency results: cells with the lowest Ho fluorescence (R7 region in the gradient) achieved equivalent engraftment at lower cell doses and therefore exhibited ≈10 times more repopulating ability than whole bone marrow (WBM). In contrast, cells having high fluorescence (R3 region in the gradient) showed a displacement of the engraftment dose-response curve to higher cell doses (Fig. 2*A*). Similar engraftment results were obtained for bone marrow c-kit and secondary long-term culture colony-forming cells (LTC-CFCs) as well as peripheral blood leucocytes at 12–14 months posttransplant (Fig. 2*B*). From these data the long-term repopulating unit (LTRU) frequencies followed the late-developing (day 28–35) but not early-developing (day 7) CAFC data. Overall, the lowest Ho perfused bone marrow fraction (R7) contained 90- to 200-fold more HSCs than the highest perfused fraction (R3) according to both *in vitro* and *in vivo* functional assays and thus indicate that the stem cells in the bone marrow are highly concentrated at the end of the Ho perfusion gradient and may therefore be located in regions of the lowest oxygen concentration.

HSCs in the Bone Marrow Are Positive for a Hypoxic Cell Marker. We and others have previously shown that bone marrow SP cells, as defined by their ability to efficiently efflux the Ho dye, are also highly enriched for HSC activity (20–24). In this case Ho staining is used in a very different manner to the *in vivo* dye perfusion study described above as the cells are exposed ex vivo to a constant concentration of Ho for a period of 90 min to allow for active dye exclusion. To detect hypoxic cells in SP and non-SP cells derived from bone marrow, we used the reductive 2-nitroimidazole compound pimonidazole (PIM) (a chemical marker for hypoxia) which, when administered *in vivo*, forms stable adducts in hypoxic regions that can then be subsequently identified with an anti-PIM antibody. We confirmed that this marker is indeed selective for hypoxic bone marrow cells by the *in vitro* treatment of isolated SP and non-SP cells with PIM (100 μM) for 5 h. Positive staining with the anti-PIM antibody was observed only under conditions of exposure to anoxia (95% N_2 with 5% CO_2) (see SI Fig. 7) and therefore was not related to hypoxia-independent differences in PIM adduct formation. Because thymus has been reported to be an hypoxic organ (25), we used thymus as a positive control in tandem with bone marrow samples for the *in vivo* detection of hypoxia. PIM (120 mg/kg) was injected i.p. and bone marrow and thymocytes were harvested after 3 h. Bone marrow cells were stained with Ho *in vitro* and SP and non-SP cells were isolated by fluorescence-assisted cell sorting (FACS). Thymocytes and sorted bone marrow populations were then stained with anti-PIM antibody and analyzed for PIM binding by flow cytometry. PIM binding was compared between saline-injected controls and PIM-injected samples. As shown in SI Figs. 5 and 8*A*, the majority of thymocytes are both hypoperfused (given the low intensity of Ho staining after dye injection) and are hypoxic (given positive staining with the anti-PIM antibody). Microscopic evaluation of thymic tissue showed PIM binding in areas of low Ho staining (see SI Fig. 8*B*). These results confirm the overall hypoxic state of thymic tissue as shown previously (25).

In the bone marrow fractions, non-SP cells demonstrated only a small shift of PIM staining as compared with the saline control mice (R1 region in Fig. 3*A*). Within SP cells, the low dye effluxing fraction (the top R2 region in Fig. 3*A*) showed increased anti-PIM

CELL BIOLOGY

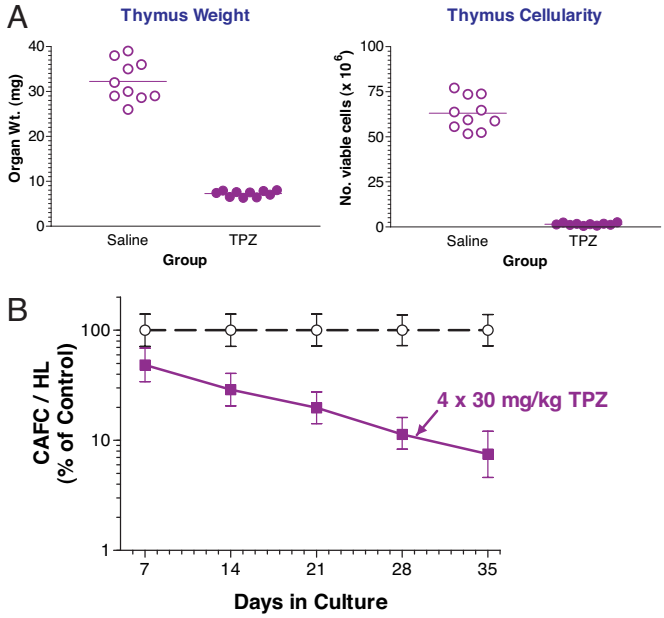

Fig. 4. The hypoxic cytotoxin TPZ is highly toxic to thymus and selectively depletes late-forming CAFCs in the bone marrow. TPZ was administered i.p. to C57BL/6J recipients in four daily doses of 30 mg/kg. On the day after the last dose, thymus and bone marrow were harvested and compared with cells obtained from saline-injected control mice. (*A*) Thymus weight (*Left*) and cell yield (*Right*) (trypan blue excluding) were estimated from three separate experiments in mice treated with 4 × 30 mg/kg over 4 days showing marked toxicity of TPZ. (*B*) Bone marrow cells were pooled from four mice and plated for estimate of CAFC content per hind limb (HL). Error bars represent 95% confidence intervals.

staining, and high dye effluxing "tip" SP cells (the bottom R3 region in Fig. 3*A*) had the highest PIM staining. The higher binding of the hypoxic marker on SP cells was also seen on microscopic evaluation of immunostained cytospin preparations (Fig. 3*B*).

Hypoxic Cytotoxin Tirapazamine (TPZ) Selectively Depletes Primitive HSCs in the Bone Marrow. Under hypoxic conditions, TPZ is reduced to a benzotriazinyl radical and other reactive intermediates that ultimately leads to DNA double-strand breaks and cell death. However, when oxygen is present, the TPZ radical is back-oxidized to the nontoxic parent compound (9). We reasoned that if many HSCs are indeed hypoxic, then these cells might be rendered sensitive to TPZ treatments. Accordingly, we administered TPZ into mice in four daily doses of 30 mg/kg and then assessed the effects of this drug on harvested bone marrow and thymocytes. As shown in Fig. 4*A*, *in vivo* TPZ treatment caused a decrease in thymic weight and cellularity, indicating that the thymus is indeed a grossly hypoxic tissue. The CAFC assay was used to evaluate the number of different hematopoietic subsets in the bone marrow after TPZ treatment (SI Table 1) from which an estimate of the surviving fraction was obtained (Fig. 4*B*). *In vivo* treatment of mice with TPZ caused a progressive loss of CAFCs with time in culture reaching ≈90% depletion of the day 35 CAFC content (HSCs). Severe depletion of cells expressing the SP phenotype was also seen after TPZ treatment with an estimated 95% loss in number of SP cells per hind limb (SI Fig. 9). In appreciating that the bioavailability of the drug and the levels of hypoxia are not directly comparable to the *in vivo* situation, the *in vitro* treatment of bone marrow suspensions with TPZ gassed with air or nitrogen for 2 h showed that the drug was only toxic under anoxic conditions and affected all CAFC subsets with even higher toxicity to the mature day-7 CAFC subset (SI Fig. 10). Thus the selective toxicity seen *in vivo* toward the more primitive CAFC subsets is therefore supportive of the HSCs being relatively more hypoxic than the progenitor descendant population.

Discussion

Using a number of experimental approaches and functional assays, we provide previously unrecognized direct evidence that HSCs in the bone marrow tissue are organized in relation to regional blood supply and level of oxygenation. Our *in vivo* application of a soluble fluorescent dye, a selective hypoxic marker and cytotoxicity of a bioreductive drug was inspired by many of the prior investigations on solid tumors in which the significance of physiological hypoxia is already well-recognized. In particular, it has been established from both flow cytometric and microscopic observations that there is reasonable concordance between an oxygen gradient and the intensity of cellular Ho staining following i.v. administration of Ho (15–18). Under the conditions of our own bone marrow studies, we were able to discount the influence of Ho dye efflux *in vivo* and to isolate different subpopulations by FACS for further assessment of HSC function according to the extent of dye perfusion *in situ*. Through the use of both *in vitro* and *in vivo* assays of long term repopulation, we were able to consistently demonstrate that HSCs are largely concentrated in regions of the bone marrow that are the least perfused with this dye. Conversely, a deficit in HSCs was observed in the upper highly perfused regions of the Ho gradient with ≈100-fold difference in late-forming CAFCs (day 35 in culture) and LTRUs (beyond 6 months after bone marrow transplantation). This relationship was confined to the most primitive of hematopoietic cells as no such distribution was seen for the descendant progenitor population measured from the short-term production of CAFCs.

The formation of PIM adducts has been shown to depend on cellular oxygen tension and has proved to be a useful marker for cells that have experienced hypoxia with $pO_2 \leq 10$ mmHg (26). The separate *in vitro* use of the Ho dye to identify SP cells has enabled us to show preferential antibody staining against PIM adducts in a population that is associated with HSC activity. Indeed, the highest anti-PIM staining was seen in the rare fraction of "tip" SP cells that is known to have the highest content of HSCs as consistently demonstrated in CAFC and long-term reconstitution experiments (21–23). In this respect, we found that parallel measurements in thymic tissue of the same mice were an important source of comparison, both in terms of validating the assays and in deriving an estimate of the level of oxygenation. In contrast to the majority of bone marrow cells, thymocytes showed gross Ho dye hypoperfusion (SI Fig. 5) and widespread staining with the PIM hypoxia marker (SI Fig. 8*B*) consistent with the previous study of Hale *et al.* (25). The intensity of staining with the anti-PIM antibody was met only by bone marrow cells isolated from the SP "tip" region (Fig. 3). The thymus is also more accessible to oxygen microelectrode measurements and pO2 values of ≈10 mmHg have been estimated (25). Thus, only the very small fraction of HSCs and closely associated cells appear to exist at around this low level of oxygen whereas most of the bone marrow tissue containing the committed and differentiating progenitors appears to be relatively well oxygenated.

Further evidence for selective HSC hypoxia comes from the survival of different hematopoietic cell subsets following the administration of the bioreductive compound TPZ. This drug was initially developed as a therapeutic agent to target hypoxic cells in tumors (9) but its effect on the primitive HSC population in the bone marrow had yet to be investigated. By discriminating short- and long-term repopulating cells in the well-validated CAFC assay (27–30) and establishing that TPZ is only toxic to these cells under hypoxia *in vitro*, we now show that HSCs are the most depleted by the *in vivo* effects of this drug (Fig. 4), although this needs to be confirmed by using the *in vivo* long-term repopulation (LTR) assay. This is in apparent contrast to preclinical studies showing only

moderate, if any, early hematological toxicity of this drug when administered as a single agent (31–33). Comparisons among a number of different chemotherapy drugs and radiation regimens have, however, shown that the loss of progenitor non-stem cell populations predominantly contributes to their acute hematological side-effects (27, 28). As the early-forming CAFC subsets (representing committed short-term repopulating CFU-C and CFU-S progenitor populations) were relatively spared by TPZ treatment then it is perhaps not surprising that the high toxicity to real long-term repopulating HSCs have been previously overlooked. Again, parallel measurements on the hypoxic thymus have provided confirmatory data by showing dramatic reduction in organ weight and cellularity after TPZ.

The stem cell niche consists of a specialized microenvironment that nurtures and regulates the stem cell pool. Previous reports have focused on the endosteal region of the bone marrow as being the principal site of the stem cell niche involved in hematopoiesis (5, 6) where the restrictive role of angiopoietin and osteopontin molecular interactions with neighboring osteoblasts have been revealed in maintaining HSC quiescence (7, 34, 35), although the association of HSCs with sinusoidal endothelium has been recently proposed as an additional or alternative site for the niche in this tissue (36). The current study now provides evidence that a relatively low level of oxygenation is also a hallmark of the bone marrow stem cell niche. Indeed, an oxygen gradient may provide a positional effect that defines the spatial organization of the hematopoietic system and confers a primary physiological role in maintaining stem cell homeostasis as well as providing a microenvironment that is protected from the toxic and mutagenic effects of oxygen-generated free radicals. As HSCs are typically noncycling with less metabolic need for oxidative respiration they can reside and function adequately in a hypoxic state. Recent quantitative proteomics analysis of isolated bone marrow populations based on cell surface markers $Lin^{-}Sca^{+}Kit^{+}$ (LSK) indicate that these cells express high levels of glycolytic and oxidative repair proteins (37). Although this particular cell population also contains a significant amount of non-stem cell progenitors and are not as highly and exclusively enriched for HSCs as "tip" SP cells (24, 38), it does indicate that at least some bone marrow cells are adapted to anaerobic metabolism. In this regard, the factors that control the SP phenotype of HSCs are particularly important as it is already known that the active efflux of the Ho dye is due to the expression of the ABC transporter ABCG2/BCRP-1 (39). Our own observation that SP cells, especially those capable of the highest Ho efflux in the "tip" region of the SP profile, are positive for the hypoxic marker PIM support the findings by Krishnamurthy *et al.* (40) where BCRP-1/ABCG2 confers a survival advantage under hypoxic conditions and, moreover, HIF-1α (a master regulator of hypoxia-induced genes) activates BCRP expression (40). Evidence also exists for control of the chemokine stromal-derived factor-1 (SDF-1 also known as CXCL12) by HIF-1α (41) leading to the interesting possibility that an inverse relationship normally exists between oxygen and SDF-1 concentration gradient, which may provide the mechanism whereby transplanted HSCs home toward the stem cell niche following extravasation at the marrow site. Notably, hypoxia-inducible transcription factors are also beginning to be appreciated to control the expression of genes associated with stem cell self-renewal including telomerase (42, 43), *Oct4* (44) and *Notch* (45) as evidenced from studies on other tissue systems. HIF proteins via their stabilization under regionally defined low oxygen tension may thus serve as upstream and dominant regulators of many key genes involved in HSC function.

In summary, we show that long-term repopulating HSCs in the mouse are relatively hypoxic consistent with their location at the lowest end of an oxygen gradient. Whether the Ho distribution represents a finite distance from blood vessels to the bone marrow endosteum or reflects regional variations in blood flow that encompasses specialized endothelial domains (36) associated with high E-selectin and SDF-1 expression (46) remains to be resolved. Recognition of the fundamental physiological role of hypoxia in HSC function and its interplay with neighboring cells of the stem cell niche will provide the groundwork for developing new strategies aimed at manipulating the growth and survival of HSCs, improving on stem cell transplantation and understanding the evolution of malignant disease in the bone marrow microenvironment.

Materials and Methods

Mice and Treatment. All animal procedures were approved by the Institutional Animal Care and Use Committee at Dana–Farber Cancer Institute. All mice were male, were obtained from Jackson Laboratories (Bar Harbor, ME) and were used in experiments between 10 and 16 weeks of age. C57BL/6J mice (CD45.2) were used as treated recipient mice. For *in vivo* repopulation assays, B6.SJL-*Ptprc*^{a} *Pep3*^{b}/BoyJ congenic mice (with the CD45.1 antigenic marker) were used as donors.

TPZ (1,2,4-benzotriazine-3-amine 1,4-dioxide, SR 4233; Sigma–Aldrich, St. Louis, MO) was dissolved in sterile PBS and injected i.p. at a dose of 30 mg/kg per day over 4 days.

Measurement of Ho Perfusion *in Vivo* in Mice. The Ho dye perfusion in mice was performed similar to that described in previous tumor studies (17–19). C57BL/6J mice were injected i.v. via the retro-orbital sinus under isoflurane anesthesia with two doses (0.8 mg/mouse) of Ho 33342 dye (Sigma, St. Louis, MO) at 10 and 5 min before bone marrow and thymus harvesting, a period that we determined was insufficient for active dye exclusion *in vitro*. Tibias and femurs were placed immediately on ice, crushed in a precooled mortar and pestle, filtered and suspended in cold Hank's balanced salt solution (HBSS) containing 2% FBS and 10 mM Hepes buffer (Gibco, Carlsbad, CA) (HBSS+). Thymus was harvested and thymocytes were also suspended in cold HBSS+. Then, 2 μg/ml propidium iodide was added to the samples and used for flow cytometric analysis and cell sorting. The dual emission wavelength of Ho fluorescence in bone marrow and thymus cell suspensions was assessed on a logarithmic scale by using flow cytometry on a dual-laser instrument (MoFlow; Cytomation, Inc., Fort Collins, CO) with exclusion of erythrocytes and propidium iodide positive cells.

Isolation of SP Cells. The bone marrow cells were stained *in vitro* with Ho 33342 (Sigma) and isolated as described by Goodell *et al.* (20). The Ho-stained bone marrow cells were stained with a phycoerythrin (PE)-labeled anti-CD45R (clone, RA3-6B2; BD PharMingen, San Diego, CA) antibody to remove cross-reactivity of the goat antibody against B-cells during anti-PIM staining.

PIM Binding. The detection of hypoxic cells in bone marrow and thymus was performed by PIM binding by using a modified intracellular staining and flow cytometric method described by Olive *et al.* (18, 19). The mice were injected i.p. with PIM hydrochloride (Chemicon International, Temecula, CA) at 120 mg/kg dose and the bone marrow and thymus harvested after 3 h postinjection. The total bone marrow or fractionated marrow cells as well as thymocytes were fixed and permeabilized by using an Intraprep Permeabilization Reagent kit (Beckman Coulter, Fullerton, CA). The cells were then stained with a mouse monoclonal anti-PIM antibody (Hypoxyprobe-1 Kit; Chemicon International, Temecula, CA) or a mouse IgG1 isotype control antibody for 1 h at 37°C in the presence of a protein blocker (DakoCytomation, Carpinteria, CA). Secondary antibody staining was performed by using Alexa Fluor 488 IgG F(ab′)2 fragment of goat anti-mouse IgG (H+L) (Molecular Probes, Invitrogen, Carlsbad, CA) in the presence of protein blocker for 30 min on ice. The cells were then analyzed for fluorescence intensity by using flow cytometry (FACScan; Becton Dickinson, Franklin Lakes, NJ) after gating on cells

with low forward- and side-scatter. Sorted cells (excluding B-lymphocytes, granulocytes and macrophages) were also centrifuged onto glass slides by using a cytospin and were then fixed and stained with the anti-PIM primary antibody and the secondary Alexa Fluor 488 antibody. Cells were counterstained with DAPI (4′,6-diamidino-2-phenylindole) to visualize nuclear DNA. Immunofluorescent images were obtained with a Nikon (Tokyo, Japan) TE-2000U inverted microscope and objective lens ×60/N.A. 1.4 coupled with a SPOT-RT digital camera. Images were processed by using PhotoShopCS.

CAFC Assay. *In vitro* determination of hematopoietic stem and progenitor cell frequencies was performed by a limiting dilution analysis of CAFC in microcultures by using the bone marrow stromal cell line FBMD-1 according to methods described (29, 30). This assay measures a spectrum of hematopoietic cells that is well-validated to compare with other functional assays. Specifically, day 7 and day 14 CAFC correspond to early progenitor cells and to CFU-spleen-day 12 cells whereas the more primitive HSC with long-term repopulating ability correspond to day 28 and 35 CAFC (30).

Long-Term Repopulation *in Vivo*. Varying numbers of bone marrow test cells from B6-CD45.1 donor mice were mixed with a 2×10^5 of non-SP supporting bone marrow cells harvested from recipient-type B6-CD45.2 mice. The mixtures were injected i.v. into groups of B6-CD45.2 recipients previously irradiated with 10 Gy (^{137}Cs γ-rays at 99.8 cGy/min). Blood samples were collected from the recipients at 18 weeks and the donor cells were determined by staining blood leukocytes with FITC-conjugated anti-CD45.1 antibody (clone A20). The percentage of donor-derived T cells, B cells and myeloid cells was determined by co-staining with PE-labeled anti-CD3e (clone 145-2C11), anti-B220 (clone RA3-6B2), and anti-Mac-1/Gr-1 antibodies (clones M1/70 and RB6-8C5), respectively, and analyzed on a FACScan instrument (Becton Dickinson, Franklin Lakes, NJ). All of the transplanted mice were killed at 12–14 months posttransplant and the donor cell chimerism in bone marrow and blood was analyzed. The bone marrow was analyzed for donor cell chimerism in c-kit$^+$ cells as well as in LTC-CFCs. The c-kit chimerism was determined by co-staining marrow cells with FITC-conjugated anti-CD45.1 antibody and PE-labeled anti-c-kit (clone ACK4) antibody. For LTC-CFCs, marrow cells were grown on FBMD-1 stromal layers for 6 weeks in culture followed by CFC growth for 9 days in methyl cellulose medium supplemented with cytokines (M3434; Stem Cell Technologies, Vancouver, BC, Canada). The cell suspensions arising from the LTC-CFC cultures were then analyzed for percentage of CD45.1 vs. CD45.2 cells by co-staining with FITC-conjugated anti-CD45.1 and biotinylated anti-CD45.2 (clone 104) antibodies followed by staining with PE-labeled streptavidin. All of the antibodies were purchased from BD PharMingen (San Diego, CA).

Statistical Analysis. For statistical analysis of *in vitro* CAFCs and *in vivo* LTRUs, the Poisson-based limiting dilution analysis calculation was used and 95% confidence limits were calculated for each subset by using L-Calc program (StemSoft Software Inc., Vancouver, BC, Canada).

We thank James Clyne and Mark Umphrey II for their superb technical assistance. This work was supported by a Joint Center for Radiation Therapy Foundation grant (to K.P.) and National Institutes of Health Grants R01CA10941 (to P.M.), U19AI067751 from the Centers for Medical Counter Measures Against Radiation (to P.M.), and R01HL073714 (to R.S.).

1. Schofield R (1978) *Blood Cells* 4:7–25.
2. Weissman IL, Anderson DJ, Gage F (2001) *Annu Rev Cell Dev Biol* 17:387–403.
3. Lord BI (1990) *Int J Cell Cloning* 8:317–331.
4. Nilsson SK, Johnston HM, Coverdale JA (2001) *Blood* 97:2293–2299.
5. Calvi LM, Adams GB, Weibrecht KW, Weber JM, Olson DP, Knight MC, Martin RP, Schipani E, Divieti P, Bringhurst FR, *et al.* (2003) *Nature* 425:841–846.
6. Zhang J, Niu C, Ye L, Huang H, He X, Tong WG, Ross J, Haug J, Johnson T, Feng JQ, *et al.* (2003) *Nature* 425:836–841.
7. Arai F, Hirao A, Ohmura M, Sato H, Matsuoka S, Takubo K, Ito K, Koh GY, Suda T (2004) *Cell* 118:149–161.
8. Thomlinson RH, Gray LH (1955) *Br J Cancer* 9:539–549.
9. Brown JM, Wilson WR (2004) *Nat Rev Cancer* 4:437–447.
10. Harris AL (2002) *Nat Rev Cancer* 2:38–47.
11. Danet GH, Pan Y, Luongo JL, Bonnet DA, Simon MC (2003) *J Clin Invest* 112:126–135.
12. Cipolleschi MG, Dello Sbarba P, Olivotto M (1993) *Blood* 82:2031–2037.
13. Ivanovic Z, Dello Sbarba P, Trimoreau F, Faucher JL, Praloran V (2000) *Transfusion* 40:1482–1488.
14. Chow DC, Wenning LA, Miller WM, Papoutsakis ET (2001) *Biophys J* 81:685–696.
15. van Laarhoven HW, Bussink J, Lok J, Punt CJ, Heerschap A, van Der Kogel AJ (2004) *Int J Radiat Oncol Biol Phys* 60:310–321.
16. Bernsen HJ, Rijken PF, Peters H, Raleigh JA, Jeuken JW, Wesseling P, van der Kogel AJ (2000) *J Neurosurg* 93:449–454.
17. Durand RE, Chaplin DJ, Olive PL (1990) *Methods Cell Biol* 33:509–518.
18. Olive PL, Durand RE, Raleigh JA, Luo C, Aquino-Parsons C (2000) *Br J Cancer* 83:1525–1531.
19. Olive PL, Luo CM, Banath JP (2002) *Br J Cancer* 86:429–435.
20. Goodell MA, Brose K, Paradis G, Conner AS, Mulligan RC (1996) *J Exp Med* 183:1797–1806.
21. Parmar K, Sauk-Schubert C, Burdick D, Handley M, Mauch P (2003) *Exp Hematol* 31:244–250.
22. Goodell MA, Rosenzweig M, Kim H, Marks DF, DeMaria M, Paradis G, Grupp SA, Sieff CA, Mulligan RC, Johnson RP (1997) *Nat Med* 3:1337–1345.
23. Matsuzaki Y, Kinjo K, Mulligan RC, Okano H (2004) *Immunity* 20:87–93.
24. Pearce DJ, Ridler CM, Simpson C, Bonnet D (2004) *Blood* 103:2541–2546.
25. Hale LP, Braun RD, Gwinn WM, Greer PK, Dewhirst MW (2002) *Am J Physiol* 282:H1467–H1477.
26. Raleigh JA, Dewhirst MW, Thrall DE (1996) *Semin Radiat Oncol* 6:37–45.
27. Down JD, Ploemacher RE (1993) *Exp Hematol* 21:913–921.
28. Down JD, Boudewijn A, van Os R, Thames HD, Ploemacher RE (1995) *Blood* 86:122–127.
29. Ploemacher RE, van der Sluijs JP, Voerman JS, Brons NH (1989) *Blood* 74:2755–2763.
30. Ploemacher RE, van der Sluijs JP, van Beurden CA, Baert MR, Chan PL (1991) *Blood* 78:2527–2533.
31. Holden SA, Teicher BA, Ara G, Herman TS, Coleman CN (1992) *J Natl Cancer Inst* 84:187–193.
32. Papadopoulou MV, Ji M, Ji X, Bloomer WD (2002) *Cancer Chemother Pharmacol* 50:291–298.
33. Gallagher R, Hughes CM, Murray MM, Friery OP, Patterson LH, Hirst DG, McKeown SR (2001) *Br J Cancer* 85:625–629.
34. Stier S, Ko Y, Forkert R, Lutz C, Neuhaus T, Grunewald E, Cheng T, Dombkowski D, Calvi LM, Rittling SR, Scadden DT (2005) *J Exp Med* 201:1781–1791.
35. Nilsson SK, Johnston HM, Whitty GA, Williams B, Webb RJ, Denhardt DT, Bertoncello I, Bendall LJ, Simmons PJ, Haylock DN (2005) *Blood* 106:1232–1239.
36. Kiel MJ, Yilmaz OH, Iwashita T, Yilmaz OH, Terhorst C, Morrison SJ (2005) *Cell* 121:1109–1121.
37. Unwin RD, Smith DL, Blinco D, Wilson CL, Miller CJ, Evans CA, Jaworska E, Baldwin SA, Barnes K, Pierce A, *et al.* (2006) *Blood* 107:4687–4694.
38. Camargo FD, Chambers SM, Drew E, McNagny KM, Goodell MA (2006) *Blood* 107:501–507.
39. Zhou S, Schuetz JD, Bunting KD, Colapietro AM, Sampath J, Morris JJ, Lagutina I, Grosveld GC, Osawa M, Nakauchi H, Sorrentino BP (2001) *Nat Med* 7:1028–1034.
40. Krishnamurthy P, Ross DD, Nakanishi T, Bailey-Dell K, Zhou S, Mercer KE, Sarkadi B, Sorrentino BP, Schuetz JD (2004) *J Biol Chem* 279:24218–24225.
41. Ceradini DJ, Kulkarni AR, Callaghan MJ, Tepper OM, Bastidas N, Kleinman ME, Capla JM, Galiano RD, Levine JP, Gurtner GC (2004) *Nat Med* 10:858–864.
42. Nishi H, Nakada T, Kyo S, Inoue M, Shay JW, Isaka K (2004) *Mol Cell Biol* 24:6076–6083.
43. Yatabe N, Kyo S, Maida Y, Nishi H, Nakamura M, Kanaya T, Tanaka M, Isaka K, Ogawa S, Inoue M (2004) *Oncogene* 23:3708–3715.
44. Covello KL, Kehler J, Yu H, Gordan JD, Arsham AM, Hu CJ, Labosky PA, Simon MC, Keith B (2006) *Genes Dev* 20:557–570.
45. Gustafsson MV, Zheng X, Pereira T, Gradin K, Jin S, Lundkvist J, Ruas JL, Poellinger L, Lendahl U, Bondesson M (2005) *Dev Cell* 9:617–628.
46. Sipkins DA, Wei X, Wu JW, Runnels JM, Cote D, Means TK, Luster AD, Scadden DT, Lin CP (2005) *Nature* 435:969–973.